



The mechanical properties of biofilm populated sand  
by Philip Gyr

A thesis submitted in partial fulfillment of the requirements for the degree of Master of Science in Civil Engineering

Montana State University

© Copyright by Philip Gyr (1998)

Abstract:

The introduction and growth of biofilm have been shown to decrease the hydraulic conductivity of sand by as much as 99 percent. This impermeable region created by biofilm forming biomass in the void spaces of porous media is known as a biobarrier. It is envisioned that biobarriers will be used for groundwater contamination containment in much the same way that grout curtains or slurry trenches are currently used. The growth of biobarriers may also prove to be an effective means of in situ bioremediation. Ongoing research at the Center for Biofilm Engineering at Montana State University-Bozeman involves the investigation of the growth, effectiveness, and sustainability of biobarriers in both plugging and remediation applications.

While bacterial plugging and bioremediation show great potential, the impact of bacterial growth on the stability and deformation characteristics of the populated medium is unknown. For biobarriers to be used safely in and under existing geotechnical structures, the effect of biofilm on soil mechanical properties must be understood. The research presented here examines the effects of one type of biobarrier on a laboratory sand.

The goal of this work was to evaluate biobarrier effects on material behavior and the performance of certain types of geotechnical structures. To quantify biofilm induced changes in mechanical properties, triaxial and one-dimensional consolidation tests were performed on populated and control samples. Due to difficulties encountered in the preparation of biobarrier samples, the only data obtained was for sand of high relative density. In this high-density sand, the addition of biofilm caused an accelerated time dependent creep rate, while other properties remained unchanged. An elasto-plastic constitutive model was calibrated using experimental data and a finite element code. The constitutive model chosen incorporates both a Drucker-Prager line and an elliptical cap as plastic yield surfaces. Creep is incorporated into the model and is dependent on the magnitude of the first stress invariant and time. The finite element code was then used to model a slope and a foundation to determine the significance of the accelerated creep rate on structural behavior. The addition of biofilm was found to cause a moderate increase of deformation in the modeled structures.

**THE MECHANICAL PROPERTIES OF BIOFILM  
POPULATED SAND**

by  
Philip Gyr

A thesis submitted in partial fulfillment  
of the requirements for the degree

of  
Master of Science  
in  
Civil Engineering

MONTANA STATE UNIVERSITY-BOZEMAN  
Bozeman, Montana

May 1998

N378  
G999

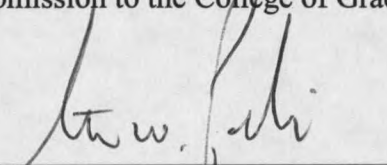
**APPROVAL**

of a thesis submitted by

Philip Gyr

This thesis has been read by each member of the thesis committee and has been found to be satisfactory regarding content, English usage, format, citations, bibliographic style, and consistency, and is ready for submission to the College of Graduate Studies.

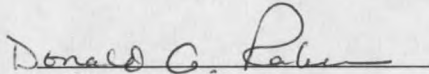
Dr. Steven W. Perkins

  
\_\_\_\_\_  
(Signature)

5-7-98  
(Date)

Approved for the Department of Civil Engineering

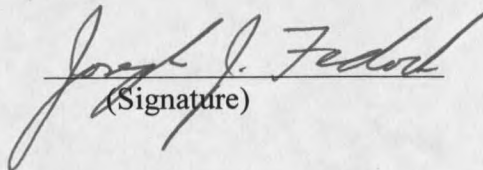
Dr. Donald Rabern

  
\_\_\_\_\_  
(Signature)

5/8/98  
(Date)

Approved for the College of Graduate Studies

Dr. Joe Fedock

  
\_\_\_\_\_  
(Signature)

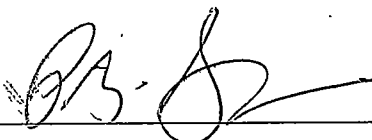
5/14/98  
(Date)

## STATEMENT OF PERMISSION TO USE

In presenting this thesis in partial fulfillment of the requirements for a master's degree at Montana State University-Bozeman, I agree that the Library shall make it available to borrowers under the rules of the Library.

If I have indicated my intention to copyright this thesis by including a copyright notice page, copying is allowable for scholarly purposes, consistent with "fair use" as prescribed in the U.S. Copyright law. Requests for permission for extended quotation from or reproduction of this thesis in whole or in parts may be granted only by the copyright holder.

Signature

A handwritten signature in black ink, appearing to be "B.S. & Co.", written over a horizontal line.

Date

7 MAY 1998

## TABLE OF CONTENTS

	Page
1. INTRODUCTION.....	1
Background.....	1
Scope of Work.....	4
2. LITERATURE REVIEW.....	6
Introduction.....	6
The Influence of Biofilm on the Mechanical Properties of Sand.....	6
Biofilms in Porous Media.....	7
Mesoscale Biobarrier Research.....	9
Constitutive Modeling.....	10
Methods of Computing Secondary Settlement.....	14
3. EXPERIMENTAL METHODS.....	17
Introduction.....	17
Triaxial Sample Preparation.....	18
Preparation of Biofilm Populated Triaxial Samples.....	21
Biobarrier Growth and Sloughing.....	23
Conventional Triaxial Compression Tests (CTC).....	28
Hydrostatic Compression.....	29
Oedometer Experiments.....	29
Preparation of Biofilm Populated Oedometer Samples.....	30
Primary Consolidation.....	32
Secondary Compression.....	33
4. EXPERIMENTAL RESULTS AND ANALYSIS.....	34
Introduction.....	34
Logarithmic Strain.....	34
Primary Consolidation.....	35
Secondary Compression.....	37
Consolidated Drained Triaxial Tests.....	39
Failure Surface.....	40

## TABLE OF CONTENTS-Continued

	Page
Strain Softening and Dilatation.....	41
Elastic Properties.....	42
Poisson's Ratio.....	42
Elastic Modulus.....	44
Consolidated Undrained Triaxial Tests.....	46
Hydrostatic Compression Tests.....	47
 5. CONSTITUTIVE MODELING.....	 49
Introduction.....	49
Model Selection.....	50
Drucker Prager Cap Model.....	50
Hardening Rule.....	51
Flow Rule.....	53
Yield Surfaces.....	54
Cap.....	54
Drucker Prager Failure Line.....	55
Overall Function of the Drucker Prager Cap Model.....	56
$K_0$ Stress Path.....	57
Triaxial Stress Path, Normally Consolidated Material.....	58
Triaxial Stress Path, Heavily Overconsolidated Material.....	61
Creep Mechanism.....	63
Calibration.....	65
Parameters Calibrated Using Data from Consolidated Drained Triaxial Tests.....	66
Triaxial Finite Element Model.....	68
Parameters Calibrated Using Oedometer Data.....	71
Oedometer Finite Element Model.....	72
Constitutive Model Limitations.....	75
Strain Softening.....	75
Dilatation.....	77
 6. FINITE ELEMENT MODELING.....	 79
Introduction.....	79
Infinite Strip Foundation.....	80
Model Composition.....	82

## TABLE OF CONTENTS-Continued

	Page
Model Loading.....	82
Model Verification.....	83
Modeling Biobarrier Insertion.....	87
Results.....	88
FEM Results.....	88
Settlements Computed Using a Conventional Method.....	91
Comparative Analysis .....	92
Slope Model.....	94
Model Composition, Loading, and Boundary Conditions.....	94
Results and Analysis.....	96
7. SUMMARY, CONCLUSIONS, AND RECOMMENDATIONS FOR FURTHER RESEARCH.....	99
Summary and Conclusions.....	99
Recommendations for Further Research.....	101
Sample Preparation and Testing.....	101
Constitutive Modeling.....	103
Elastic and Plastic Parameters.....	104
Creep in Compression.....	104
Finite Element Modeling.....	105
REFERENCES CITED.....	107
APPENDIX: EXPERIMENTAL RESULTS.....	110

## LIST OF TABLES

Table	Page
3.1 Composition of nutrient solution.....	22
3.2 Hydraulic conductivity reduction in 65% relative density samples.....	24
3.3 Hydraulic conductivity reduction in 100% relative density samples.....	26
3.4 Bacterial populations in triaxial samples.....	27
3.5 Bacterial population in oedometer samples.....	32
5.1 Creep parameters.....	74
6.1 Foundation Settlements.....	92
6.2 Strains for portions of the slope surface.....	98

## LIST OF FIGURES

Figure	Page
2.1 Column Biobarrier apparatus.....	10
2.2 Drucker Prager model.....	11
2.3 Sandler's Cap model.....	12
3.1 Triaxial mold, cutaway views.....	19
3.2 Falling head permeability apparatus.....	20
3.3 Hydraulic conductivity reduction in a column biobarrier.....	23
3.4 Modified oedometer ring a) top view, b) side view.....	31
4.1 Results from primary consolidation tests.....	37
4.2 Typical secondary compression data.....	38
4.3 Average creep slope for each load step.....	39
4.4 $p$ - $q$ diagram showing ultimate strengths, $\beta$ and failure line.....	41
4.5 Strain softening and dilation in a CD-CTC test with 300 kPa confinement.....	43
4.6 Deviator stress vs. axial strain showing initial elastic region in a CD-CTC test with 300 kPa confinement .....	43
4.7 Average modulus values.....	44
4.8 Axial stress versus strain curves showing reduced elastic modulus for biobarriers in a CD-CTC test with 300 kPa confinement.....	46
4.9 CU-CTC results at a 300 kPa confinement.....	47

## LIST OF FIGURES-Continued

Figure	Page
4.10 Hydrostatic compression data.....	48
5.1 Drucker Prager Cap model; yield surfaces and elastic region.....	51
5.2 Hardening rule.....	52
5.3 Flow potential surface, plastic strain vector and components.....	54
5.4 Flow potential surfaces and plastic strain vectors.....	56
5.5 $K_o$ stress path showing the plastic potential vector and it's components.....	58
5.6 Triaxial stress path, normally consolidated material.....	59
5.7 Axial and volumetric behavior of a DPC material in triaxial shear.....	60
5.8 Initial stress increment, heavily consolidated material.....	61
5.9 Second axial strain increment showing the softened cap position.....	62
5.10 Axial and volumetric behavior of an overconsolidated DPC material in triaxial shear.....	63
5.11 Creep potential surfaces and vectors.....	65
5.12 Finite element model of triaxial shear.....	68
5.13 Axial stress versus axial strain, 300 kPa confinement.....	70
5.14 Axial stress vs. axial strain, 600 kPa confinement.....	70
5.15 Volumetric straing vs. axial strain, 300 kPa confinement.....	71
5.16 Finite element model of oedometer conditions.....	73

## LIST OF FIGURES-Continued

Figure	Page
5.17 Calibration results, control sand.....	74
5.18 Calibration results, biobarrier sand.....	75
5.19 Strain softening and dilation during shear in a CD-CTC test with 300 kPa confinement.....	76
6.1 Finite element model showing one-meter wide foundation loaded to 350 kPa.....	81
6.2 Geometry and parameters used in analytical solutions.....	84
6.3 FEM and analytical solutions for vertical displacement.....	85
6.4 FEM and analytical solutions for vertical stress below centerline.....	86
6.5 FEM and analytical solutions for hydrostatic stress below centerline.....	86
6.6 Creep and total strain development with time .....	88
6.7 Vertical displacement of a one-meter foundation under 350 kPa load.....	89
6.8 Vertical displacement of a one-meter foundation under 200 kPa load.....	90
6.9 Vertical displacement of a two-meter foundation under 200 kPa load.....	90
6.10 $C_\alpha$ values.....	91
6.11 Finite element model of slope.....	95
6.12 Magnified slope settlements.....	97
6.13 Slope segments analyzed for differential strain.....	98

## LIST OF FIGURES-Continued

Figure	Page
Figure A1 Grain size distribution of F-110 Ottawa sand.....	111
Figure A2 Axial strain vs. deviator stress, 100% relative density control sand, 50 kPa confinement, CD-CTC tests.....	111
Figure A3 Axial strain vs. volumetric strain, 100% relative density control sand, 50 kPa confinement, CD-CTC tests.....	112
Figure A4 Axial strain vs. deviator stress, 100% relative density biobarrier sand, 50 kPa confinement, CD-CTC tests.....	112
Figure A5 Axial strain vs. volumetric strain, 100% relative density barrier sand, 50 kPa confinement, CD-CTC test.....	113
Figure A6 Axial strain vs. deviator stress, 100% relative density control sand, 300 kPa confinement, CD-CTC tests.....	113
Figure A7 Axial strain vs. volumetric strain, 100% relative density control sand, 300 kPa confinement, CD-CTC tests.....	114
Figure A8 Axial strain vs. deviator stress, 100% relative density biobarrier sand, 300 kPa confinement, CD-CTC tests.....	114
Figure A9 Axial strain vs. volumetric strain, 100% relative density biobarrier sand, 300 kPa confinement, CD-CTC tests.....	115
Figure A10 Axial strain vs. deviator stress, 100% relative density control sand, 600 kPa confinement, CD-CTC tests.....	115
Figure A11 Axial strain vs. volumetric strain, 100% relative density control sand, 600 kPa confinement, CD-CTC tests.....	116
Figure A12 Axial strain vs. deviator stress, 100% relative density biobarrier sand, 600 kPa confinement, CD-CTC tests.....	116

## LIST OF FIGURES-Continued

Figure	Page
Figure A13 Axial strain vs. volumetric strain, 100% relative density biobarrier sand, 600 kPa confinement, CD-CTC tests.....	117
Figure A14 Axial strain vs. deviator stress, 100% relative density control sand, 300 kPa confinement, CU-CTC tests.....	118
Figure A15 Axial strain vs. pore pressure, 100% relative density control sand, 300 kPa confinement, CU-CTC tests.....	118
Figure A16 Axial strain vs. deviator stress, 100% relative density biobarrier sand, 300 kPa confinement, CU-CTC tests.....	119
Figure A17 Axial strain vs. pore pressure, 100% relative density biobarrier sand, 300 kPa confinement, CU-CTC tests.....	119
Figure A18 $p'-q$ diagram showing peak strengths of CU-CTC and CD-CTC tests.....	120
Figure A19 Axial strain vs. deviator stress, 65% relative density biobarrier sand, 50 kPa confinement, CD-CTC test .....	120
Figure A20 Axial strain vs. volumetric strain, 65% relative density biobarrier sand, 50 kPa confinement, CD-CTC test.....	121
Figure A21 Axial strain vs. pore pressure, 65% relative density control sand, 50 kPa confinement, CD-CTC test.....	121
Figure A22 Axial strain vs. deviator stress, 65% relative density control sand, 50 kPa confinement, CD-CTC test.....	122
Figure A23 Axial strain vs. deviator stress, 65% relative biobarrier control sand, 300 kPa confinement, CD-CTC test.....	122
Figure A24 Axial strain vs. volumetric strain, 65% relative density biobarrier sand, 300 kPa confinement, CD-CTC test.....	123

LIST OF FIGURES-Continued

Figure	Page
Figure A25 Axial strain vs. deviator stress, 65% relative density control sand, 300 kPa confinement, CD-CTC test.....	123
Figure A26 Axial strain vs. volumetric strain, 65% relative density control sand, 300 kPa confinement, CD-CTC test.....	123

## ABSTRACT

The introduction and growth of biofilm have been shown to decrease the hydraulic conductivity of sand by as much as 99 percent. This impermeable region created by biofilm forming biomass in the void spaces of porous media is known as a biobarrier. It is envisioned that biobarriers will be used for groundwater contamination containment in much the same way that grout curtains or slurry trenches are currently used. The growth of biobarriers may also prove to be an effective means of in situ bioremediation. Ongoing research at the Center for Biofilm Engineering at Montana State University-Bozeman involves the investigation of the growth, effectiveness, and sustainability of biobarriers in both plugging and remediation applications.

While bacterial plugging and bioremediation show great potential, the impact of bacterial growth on the stability and deformation characteristics of the populated medium is unknown. For biobarriers to be used safely in and under existing geotechnical structures, the effect of biofilm on soil mechanical properties must be understood. The research presented here examines the effects of one type of biobarrier on a laboratory sand.

The goal of this work was to evaluate biobarrier effects on material behavior and the performance of certain types of geotechnical structures. To quantify biofilm induced changes in mechanical properties, triaxial and one-dimensional consolidation tests were performed on populated and control samples. Due to difficulties encountered in the preparation of biobarrier samples, the only data obtained was for sand of high relative density. In this high-density sand, the addition of biofilm caused an accelerated time dependent creep rate, while other properties remained unchanged. An elasto-plastic constitutive model was calibrated using experimental data and a finite element code. The constitutive model chosen incorporates both a Drucker-Prager line and an elliptical cap as plastic yield surfaces. Creep is incorporated into the model and is dependent on the magnitude of the first stress invariant and time. The finite element code was then used to model a slope and a foundation to determine the significance of the accelerated creep rate on structural behavior. The addition of biofilm was found to cause a moderate increase of deformation in the modeled structures.

## CHAPTER ONE

### INTRODUCTION

#### Background

The introduction and growth of biofilm in granular media have been shown to affect the media's hydrodynamic characteristics. Hydraulic conductivity in media consisting of 1-mm glass spheres and fine silica sand has been reduced by more than 98% with the successful introduction of biofilm forming bacteria (Cunningham et al., 1991; Shaw et al., 1985). Of particular interest are starved bacterial cells, which are much smaller than normal vegetative cells. These dormant cells are known as ultramicrobacteria (UMB). In experiments, the UMB have been transported into the micropore spaces of geologic strata then revived by continuous or dose stimulation with nutrient. Revival of the bacteria results in the production of extra cellular polymeric substances (EPS), which acts to plug the formation containing the bacteria. Research is currently being conducted within the Center for Biofilm Engineering (CBE) at MSU-Bozeman to examine the use of these bacteria in the field as biobarriers. A biobarrier wall would be used much in the same way that grout curtains or slurry trenches are currently used for containment of contaminated groundwater. The use of biobarriers for the dual

function of containment and bioremediation is also being investigated (Center For Biofilm Engineering, 1996).

Proposed applications of bioremediation typically focus on the ability of microorganisms to perform some kind of transformation and/or degradation of contaminants. A wide range of contaminants including petroleum hydrocarbons, pesticides, chlorinated solvents, heavy metals, cyanide, and radionuclides have been shown to be effectively degraded, transformed, or otherwise removed by microbial processes. Factors affecting formation and persistence of microbial biobarriers are currently being investigated at the CBE using column and lysimeter devices. These biobarriers have significantly reduced hydraulic conductivity and the flux of contaminants such as cesium and trichloroethylene.

While bacterial plugging shows great potential in containing contaminated groundwater plumes, it is not clear what the impact of bacteria will be on the stability and deformation characteristics of the populated soil medium. The purpose of this research is to examine the impact of bacteria on the mechanical properties of a fine silica sand. The effects that were anticipated are listed below:

1. The addition of a cohesive component of strength due to the exopolysaccharide produced by the bacteria and its tendency to adhere to sand particles and thereby cause particles to cohere to one another.
2. Reduced frictional component of strength caused by the addition of lubrication provided by the biofilm. It is anticipated that this lubrication

would decrease the mineral-to-mineral sliding component of friction, leaving the dilational component relatively unchanged.

3. The highly viscous properties of the biofilm populated pore fluid may add a viscous component of deformation previously unseen in the nearly inviscid clean sand.
4. Permeability reduction caused by biofilm creates a change in the pore fluid pressure response for conditions where the pore fluid is allowed to drain from the specimen for a given rate of load application. The time necessary for the pore fluid pressure, induced by an increment of load, to dissipate to drainage boundaries is dependent on the soil-pore fluid permeability. This induced pore fluid pressure in turn affects overall strength development. In other words, the lower permeability biofilm-populated sand may tend to shear in a more undrained fashion as compared to the non-populated sand for a given rate of load application.

At sites where buildings, liquid waste containers, or slopes overlie the intended biobarrier location, biofilm induced changes in soil properties could deleteriously affect performance of the structure. This thesis details efforts to determine how the addition of biofilm to laboratory sand affects the mechanical properties of the sand and geotechnical structures built on or with the sand.

### Scope of Work

The goal of this work was to evaluate biobarrier effects on material behavior and geotechnical structure performance. To accomplish this a visco-elastic-plastic constitutive model of a porous material was calibrated using experimental data in conjunction with a finite element code. A course of experimentation was planned and executed to obtain material parameters necessary to calibrate the constitutive model and quantify biofilm induced changes. The finite element code was then used to model a slope and a foundation to determine the significance of biofilm induced changes on structure behavior.

### Experimentation

A number of biobarriers had been grown and analyzed at the CBE. These biobarriers were formed by the UMB *Klebsiella oxytaca* grown in F-110 Ottawa sand. Because this reference data existed, the same combination of microbe and soil medium was selected for mechanical testing. It should also be noted that F-110 Ottawa sand is readily available and has nearly identical physical properties from batch to batch. Thus it is ideal for mechanical experimentation. The techniques used to grow biobarriers at the CBE were the basis for those used to grow biobarriers for mechanical testing. Equipment was designed and constructed to grow biobarriers in the small samples required for this purpose.

Constitutive models of sand are typically elastoplastic or viscoelastic-plastic. Parameters for both types of models are calibrated using triaxial tests. The experimental work performed consisted of drained and undrained triaxial tests. In addition, one-dimensional consolidation (oedometer) tests were performed to ascertain if biofilm induced accelerated creep behavior. These experiments were performed at different relative soil densities on biofilm and control samples.

### Modeling

An visco-elasto-plastic Drucker-Prager cap constitutive model was selected and calibrated with the assistance of a commercial finite element (FE) code called ABAQUS<sup>TM</sup>. This model incorporates elastic, plastic, and creep behaviour. Calibration consisted of modeling oedometer and triaxial tests and choosing the parameters of the constitutive model such that computer generated stresses and strains duplicated those recorded from experiment.

Once calibrated, the FE code was used to model a strip foundation and an infinite slope. The effects of a biobarrier on these structures at different load levels and over different time spans were analyzed using the results from the FE models.

## CHAPTER TWO

### LITERATURE REVIEW

#### Introduction

The literature review contained in this chapter is divided into four main sections: the influence of biofilm on sand, biobarrier research, the constitutive modeling of dense sand, and mechanisms for secondary compression in granular materials.

#### The Influence of Biofilm on the Mechanical Properties of Sand

At the time of this writing, the author is not aware of any prior research effort to examine the effects of the introduction of biofilm on the mechanical properties of soils. Research has been conducted to examine the effects of highly viscous pore fluids on the shear strength of sands (Zeng et al., 1998, Bielby, 1989). In these studies, glycerin-water mixtures and silicon oils having a viscosity approximately 80 times that of water were used as the pore fluid in a series of drained triaxial shear tests. It was concluded that the highly viscous fluid had little effect on the material properties of sand in both cases.

### **Biofilms in Porous Media**

Biofilms form when aqueous microbial cells adhere to a surface and secrete EPS. Microbial biofilms accumulate because of microbial abilities to adsorb, metabolize, and replicate on surfaces. At some point in the sorption process, a bacterial cell may become irreversibly adsorbed. Irreversible adsorption or chemisorption may involve short-range forces such as dipole-dipole interactions, dipole-induced dipole interactions, ion-dipole interactions, hydrogen bonding, hydrophobic interactions, or polymeric bridging. EPS produced at the cell surface are the adhesions most often implicated as the agents of irreversible adsorption (Characklis and Marshall, 1990). A summary of the various functions of EPS in cell-surface interactions can be found in Robb (1984).

Fundamental rate processes including growth, product formation (e.g., EPS), maintenance and/or endogenous decay, and death and/or lysis of cells control biofilm formation (Characklis and Marshall, 1990). The processes of growth and maintenance consume energy so that if nutrients become depleted, death and/or lysis occurs.

The first detailed study of the transport and growth of bacteria in porous media occurred in 1984 (Shaw et al., 1985). This study found that fully vegetative natural bacteria formed a skin plug at the inlet of the glass spheres that composed the porous media. The naturally occurring or "wild type" bacteria adhered so readily to the glass that the biobarrier formed achieved a thickness of only a few hundred microns. From this study, it was concluded that metabolically active "wild type" bacteria do not penetrate deeply into porous material.

When subjected to starvation, some bacterial cells undergo radical size reduction and adopt a dormant metabolism. These dormant cells, called ultramicrobacteria or UMB, can survive for many years. (Kjelleberg, 1993). When exposed to a nutrient rich environment, UMB are capable of rapidly resuscitating to the vegetative state. The discovery of UMB in the deep terrestrial subsurface indicates that they are capable of movement in porous media with a permeability of greater than 150 milliDarcies. UMB are not motile, therefore they are found along the path of groundwater flow in the subsurface environment.

Several researchers have performed experiments proving that UMB can be transported throughout a porous media and subsequently resuscitated. Large numbers of UMB have been shown to be retained in pore spaces as they are transported through porous media. Resuscitation has been accomplished by adding a nutrient chaser to the water flowing through the media. When the cells return to the vegetative state in a nutrient rich environment, large amounts of EPS are produced, reducing permeability (MacLeod et al., 1988, Cusack et al., 1992). Microscopic observations of fluid flow through biofilm populated porous media revealed that biofilm reduces hydraulic conductivity by blocking or restricting flow channels (Stoodley et al., 1994). The process of resuscitation and subsequent reduction in permeability are dependent on the type of UMB, the type of nutrient, and the rate of supply of the nutrient. Therefore, it is possible to grow biobarriers at selected locations within a porous media by controlling the injection and resuscitation protocols (Cunningham et al., 1997).

### Mesoscale Biobarrier Research

In recent years, the formation and persistence of biobarriers has been studied extensively at the Center for Biofilm Engineering at Montana State University, Bozeman. Biobarriers were grown in mesoscale columns and lysimeters using a variety of sands and microbes. To evaluate persistence, fully developed biobarriers were subjected to starvation and exposed to several contaminants. The protocols used in this research were the basis for the techniques used to grow biobarriers in samples used for geotechnical testing during this research.

Column barriers were formed in 6" x 36" sand-packed columns equipped with sampling and piezometer ports along the length of the flow-path. The apparatus used in these experiments is illustrated in Figure 2.1. The columns were inoculated with a solution containing the UMB *Klebsiella oxytaca*, after which nutrient was added to the influent supply initiating resuscitation and bacterial growth. Initially (0-50 days), a rapid reduction in overall hydraulic conductivity of 73% to 95% was observed. This initial plugging occurred in a gradient through the column with the greatest hydraulic conductivity reduction near the column inlet. In areas further from the column inlet, hydraulic conductivity continued to decrease slowly over time. After approximately 150 days, the reduction in hydraulic conductivity became uniform throughout the column. Exposure of established biobarriers to relevant concentrations of heavy metals (1 ppm strontium or cesium) and a chlorinated organic solvent (50-300 ppm carbon tetrachloride) did not have a deleterious effect on biobarrier integrity. The presence of microbial barriers reduced contaminant flux by 96-99% (Cunningham et al., 1997). The geometry

of the samples prepared for testing was cylindrical; therefore, data from column biobarriers was used as a benchmark for biobarrier performance in this research.

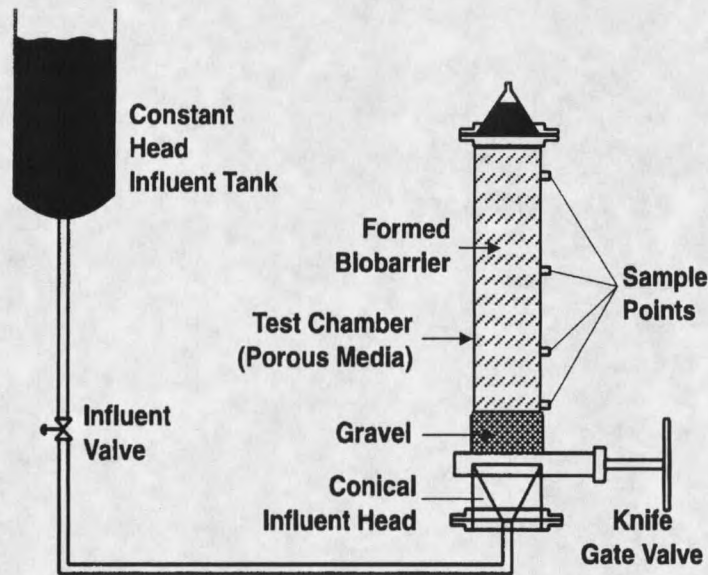


Figure 2.1 Column Biobarrier apparatus

### Constitutive Modeling

Various elasto-plastic constitutive models have been proposed to describe the material properties of granular materials. In these models, plastic behavior is described by a yield function describing the onset of plastic flow as a function of stress state and path, a flow rule describing the development of plastic strains and a hardening rule describing the change in size of the yield surface. In recent years, more complex constitutive models have been formulated that incorporate time dependence in the plastic flow rules. The Drucker-Prager Cap model used in this research is an example of this type of model.

Drucker and Prager (1952) developed the first elasto-plastic constitutive model used to describe granular material behavior. In the model, associated plastic flow occurs on a generalized Mohr-Coulomb failure line, known as the Drucker-Prager (DP) line as illustrated in Figure 2.2. The DP line is defined in a stress space with axes corresponding to the square root of the second stress invariant,  $J_2$ , and the first stress invariant,  $J_1$ . In this model, material behavior is assumed to be independent of the third stress invariant. The angle  $\alpha$  is dependent on the angle of friction and  $k$  is proportional to the cohesion. Behavior in the elastic region is governed by constant shear and bulk moduli (Drucker and Prager, 1952). The model has the following shortcomings: 1) the amount of dilatancy predicted during shear is greater than experimentally observed dilation and 2) plastic compaction caused by hydrostatic stress is not described.

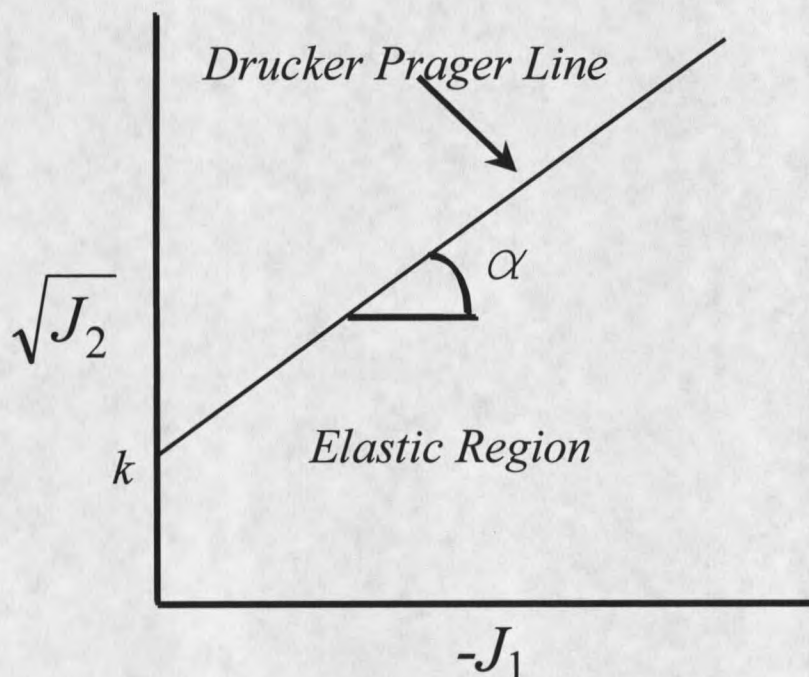


Figure 2.2 Drucker Prager model

































































































































































































































